Article

Title: Maintenance of adaptive dynamics in a bottlenecked range-edge population that retained outcrossing

Authors: Margarita Takou[1], Tuomas Hämälä[2], Kim A. Steige[1], Evan Koch[3], Hannes Dittberner[1], Levi Yant[4], Mathieu Genete[5], Shamil Sunyaev[3], Vincent Castric[5], Xavier Vekemans[5], Outi Savolainen[6], Juliette de Meaux[1]

[1] Institute of Botany, University of Cologne, Cologne, Germany

[2]Department of Plant and Microbial Biology, University of Minnesota, St. Paul, Minnesota, USA.

[3]Department of Biomedical Informatics, Harvard Medical School, Boston, Massachusetts, USA.

[4]School of Life Sciences, University of Nottingham, Nottingham NG7 2RD, UK

[5]Univ. Lille, CNRS, UMR 8198 - Evo-Eco-Paleo, F-59000 Lille, France

[6]Department of Ecology and Genetics, University of Oulu, FIN-90014 Oulu, Finland

Abstract:

During range expansion, edge populations are expected to face increased genetic drift, which in turn can alter and potentially compromise adaptive dynamics, preventing the removal of deleterious mutations and slowing down adaptation. In plants, range expansion is often concomitant with a shift in mating system. In the Northern American subspecies *Arabidopsis lyrata* ssp *lyrata*, range expansion has been associated with the evolution of a mixed mating system and the accumulation of a burden of deleterious mutations in individual genotypes. Here, we contrast populations of the European sister subspecies *Arabidopsis lyrata* ssp *petraea*, which expanded its European range without a shift in mating system. We document a sharp decline in effective population size in the range-edge population and observe that non-synonymous variants segregate at higher frequency. Yet, the time since the bottleneck was too short to allow the accumulation of a detectable per-individual genomic burden of deleterious mutations in the Northern population. We further observe that the allelic diversity at the self-incompatibility locus, which ensures strict outcrossing, has remained unchanged. Genomic footprints indicative of selective sweeps were broader in the Northern population but not less frequent. This indicates that, despite a dramatic bottleneck, adaptive mutations were present in sufficient number and effect size to maintain adaptive dynamics at the range-edge of the strictly outcrossing species *Arabidopsis lyrata* ssp. *petraea*.

Keywords: range expansion, adaptation, mutation burden, self-incompatibility locus, negative frequency-dependent selection, selective sweeps

Introduction

Range expansion events, like the postglacial colonization of Northern Europe and Scandinavia from Southern refugia, have had wide influence on the distribution of genetic diversity within species (Hewitt 2000). Through its impact on multiple population genetic processes, range expansion has cascading effects on adaptive dynamics (Excoffier et al. 2009). Indeed, it increases drift (Hallatschek et al. 2007), and leads to both a progressive loss of genetic diversity and increased levels of population differentiation along the expansion route(Austerlitz et al. 1997; Corre and Kremer 1998; Muller et al. 2008; Excoffier et al. 2009; Slatkin and Excoffier 2012) . The removal of deleterious mutations becomes less efficient and fitness is expected to decrease at the front of the species expanding range, causing what is known as the expansion load, an effect that can persist in the new population for thousands of generations. The majority of those mutations remain in low frequencies, but some can reach fast fixation, a phenomenon sometimes termed allele surfing (Klopfstein et al. 2006; Peischl et al. 2013).

Expansion load is expected to significantly interfere with adaptive dynamics. Locally adapted populations that move out of their core range are expected to evolve towards new adaptive peaks (Colautti and Barrett 2013; Savolainen et al. 2013; Wos and Willi 2018). In a population carrying an expansion load, larger adaptive steps might be required to establish a novel range edge, resulting in a slowdown of expansion, especially when dispersal is limiting (Henry et al. 2015). Theoretical studies report complex interactions among parameters such as the strength and heterogeneity of selection, the rate of expansion, as well as the architecture of traits under selection. However, to the best of our knowledge, these predictions remain untested in natural populations. In heterogeneous environments, expansion can occur if many small effect mutations affecting polygenic traits confer high enough fitness variance to the population (Gilbert et al. 2017). The same rate of expansion, however, can be reached in less diverse populations if a few large effect beneficial mutations arise (Gilbert et al. 2017). In the presence of a high expansion load, maladapted populations established at the range-edge are more likely to go extinct (Gilbert et al. 2017). The necessity to first adapt locally will thus slowdown the rate of range expansion, thereby reducing the expansion bottleneck itself (Gilbert et al. 2017). Conversely, populations at the range edge may show a comparatively increased average fitness, because they are the ones that have overcome maladaptation by adapting to the local environment. In addition, the failure to maintain an intact range core with a pool of non-deleterious alleles that can migrate to the edge can also compromise the ability of edge populations to recover from expansion load (Gilbert et al. 2018). Expansion rate and adaptive requirements therefore jointly modulate the burden individuals will accumulate at the range edge (Gilbert et al. 2017, Gilbert et al. 2018).

The speed of range expansion can also be limited by species interactions, if these are necessary for reproductive success and survival (Louthan et al. 2015). Many flowering plants rely on insects for

pollination and thus fertility (Gibbs 2014). As species expand their range, efficient pollinators can become rare, and a shift towards selfing may help restore reproductive assurance and avoid Allee effects (Jain 1976; Morgan et al. 2005; Gascoigne et al. 2009). Such a transition to selfing or mixed-mating systems has often been associated with range expansion (Goodwillie et al. 2005; Levin 2010; Laenen et al. 2018; Baker 1995 but see Cheptou 2012). However, mating system shifts can compromise adaptive processes by exposing populations to inbreeding depression and loss of genetic diversity as they face stress at the margin of their ecological niche (Slatkin 1995; Ingvarsson 2002; Barrett 2003; Glémin and Ronfort 2013). Yet, increases in the selfing rate can also contribute to the purging of deleterious mutations (Pujol et al. 2009; Glémin and Ronfort 2013; Hadfield et al. 2017) and promote the emergence of high fitness individuals at the front range of expansion (Klopfstein et al. 2006). In fact, selfing species generally show the greatest overall range size (Grossenbacher et al. 2015). In this context, plant species that have maintained a strictly outcrossing mating system across their expanded distribution range are particularly intriguing.

Arabidopsis lyrata forms two distinct subspecies, *A. l. ssp. petraea* and *A. l. ssp. lyrata,* that have expanded their range independently in two continents, and display contrasted mating system evolution (Koch 2019). Self-incompatibility (SI) in this species is achieved via the multiallelic S-locus specific to the Brassicaceae family (Bateman 1955; Kusaba et al. 2001). Phylogenetic and genomic analyses of the S-locus in the Brassicaceae have shown that strong negative frequency-dependent selection maintained S-allele lineages shared across species (Dwyer et al. 1991; Vekemans et al. 2014). The loss of SI and thus selfing, however, evolves repeatedly in the family (Tsuchimatsu et al. 2012; Vekemans et al. 2014; Durvasula et al. 2017). In the North American subspecies *A. l. ssp. lyrata,* selfing lineages have evolved multiple times at the range margin and the transition to selfing has been recently associated with a sharp decrease in average population fitness (Mable et al. 2005; Griffin and Willi 2014; Willi et al. 2018). Microsatellite data has shown that the European subspecies *A. l. ssp. petraea* also expanded its range northward after the last glaciation, but it maintained a functional SI system (Clauss and Koch 2006; Schierup et al. 2006; Koch 2019). However, northern populations in *A. l. ssp. petraea* show strong reduction in diversity (Wright et al. 2003; Muller et al. 2008; Ross-Ibarra et al. 2008; Pyhäjärvi et al. 2012; Mattila et al. 2017). Forced selfing in the *A. l. ssp. petraea* subspecies is also known to result in inbreeding depression (Kärkkäinen et al. 1999; Sletvold et al. 2013). Furthermore, there is clear evidence that *A. l. ssp. petraea* populations at the Northern range edge are locally adapted. Reciprocal transplant experiments across four sites forming a gradient from core to range margin areas in Europe indicated that the decrease in fitness away from the species core niche was less pronounced for individuals originating from the range margin (Vergeer and Kunin 2013). Reciprocal transplant studies between the Northern and Central European populations further confirmed that Northern populations have the highest survival rate in their location of origin consistent with signals of local adaptation (Leinonen et al. 2009). Major developmental traits such as

flowering time seem to have been targets of natural selection (Sandring et al. 2007; Toivainen et al. 2014; Mattila et al. 2016; Hämälä et al. 2018). Phenotypic differences in flowering time and especially selection related to the photoperiodic pathway, or to development have been shown to contribute to local adaptation in northern populations of *A.l. ssp. petraea* (Toivainen et al. 2014; Mattila et al. 2016; Hämälä and Savolainen, 2019), and response to abiotic factors such as cold and drought (Vergeer and Kunin 2013; Davey et al. 2018).

To gain insight into the combined effects of demographic history and selection processes in an outcrossing range-edge population, we quantified the demographic impact of range expansion in a Northern population of the sub-species *A. l. ssp. petraea* and examined whether its response to both negative and positive selection were impacted. We compare this population to two populations representative of the core of the species range and specifically ask: i) can we document a decreased efficacy of negative selection in the range-edge population and an increase in individual mutational burden?, ii) does the range-edge population show a decrease in S-allele diversity as expected by an ongoing mating system shift?, and iii) do we detect a slowdown of adaptive dynamics in range-edge *A. l. ssp. petraea* populations ?

We document a strong bottleneck and increased frequency of non-synonymous variants indicative of progressive range expansion. However, the per individual number of deleterious mutations has not significantly increased. We further observe that negative frequency-dependent selection on S-alleles has remained efficient and find no evidence that the response to positive selection is impaired in the range-edge population. The outcrossing subspecies *A. l.* ssp *petraea* shows a strong resilience to the effect of range expansion.

Results

Demographic history of three European *A. lyrata ssp. petraea* populations confirms a scenario of expansion

We analyzed whole genome sequence data for 46 *Arabidopsis lyrata* individuals, of which, 22 were collected in a range edge population in Norway (Spiterstulen, SP), and 17 and 7 individuals from two core populations in Germany (Plech, PL) and Austria (a scattered sample, AUS; Fig S1) respectively. We first examined the partitioning of genome-wide genetic variation along principle components. The populations of origin were clearly separated on the first two axes. The first principal component (PC) explained 24.95% of the variance, separating the Northern site from the two Central European sites (PL and AUS). The second PC (6.82%) differentiated the AUS and PL sites. AUS individuals were more scattered than SP individuals, presumably because AUS individuals were collected over a broader area (see methods, Fig 1a). Within populations, nucleotide diversity was estimated as the average number of pairwise differences per sites (π) across non-overlapping 10 kb windows. Mean

nucleotide diversity of the genomic windows was π=0.0081, π=0.0067 and π = 0.0055 for PL, AUS and SP, respectively (Table S1).

Estimates of pairwise F_{ST} corroborated the Principal Component Analysis (PCA) results. We calculated F_{ST} across 10 kb non-overlapping windows along the genome. Mean F_{ST} was 0.231 (median of 0.232) and 0.234 (median of 0.236) for SP vs. PL or AUS, respectively. Between PL and AUS, differentiation was much lower, with a mean F_{ST} value of 0.079 (median of 0.047). Most of the genetic differentiation resides between Northern and Central European populations and not between PL and AUS, which are geographically more close to each other. Average number of nucleotide differences between pairs of individuals from distinct sites (d_{xy}) confirmed the pattern of inter-population differentiation (Table S1).

Likewise, admixture analysis showed that our samples are best described with K=2 clusters (cross-validation error, cv = 0.397). The SP individuals formed a unique cluster, while PL-AUS individuals grouped together in one cluster. The second most probable scenario (cv = 0.419) was K=3, with each population forming its own cluster (Fig S2).

PCA, F_{ST} and admixture analyses measure genetic differentiation and cannot separate the effects of population history, migration and population size change. We thus used our whole genome dataset to model the demographic history of the three populations with *fastsimcoal2*. In contrast to PCA and F_{ST}, which indicated that PL and AUS are equally distantly related to SP, model selection based on the Akaike information criterion (AIC) indicated that it was significantly more probable that the ancestral population of SP and PL (SP, PL) split from the AUS lineage first (Fig 1b; Table S2). Divergence between (SP, PL) and AUS (T) was estimated to have occurred approximately 372,701 generations ago (CI: 182,494 – 526,018). The split between SP and PL was estimated to have occurred more recently, approximately T = 26,902 generations ago (CI: 20,172 – 50,778). Demographic modelling further indicated that the most probable migration scenario entailed historical migration between all populations (Table S3). The model indicated that gene-flow was five times higher between PL and AUS (PL to AUS, $4N_em$ =2.689, (CI: 0.849 – 4.825) and from AUS to PL $4N_em$= 0.214 (CI: 0.109-1.420)) than between SP and PL (SP to PL $4N_em$ = 0.829 (CI: 0.261 – 2.257), and PL to SP $4N_em$ = 0.072, (CI: 0.025 – 0.604)). Hence, the discrepancy between the observation of moderate population differentiation between PL and AUS despite long historical divergence, may apparently be explained by the maintenance of high gene flow between these Central European populations.

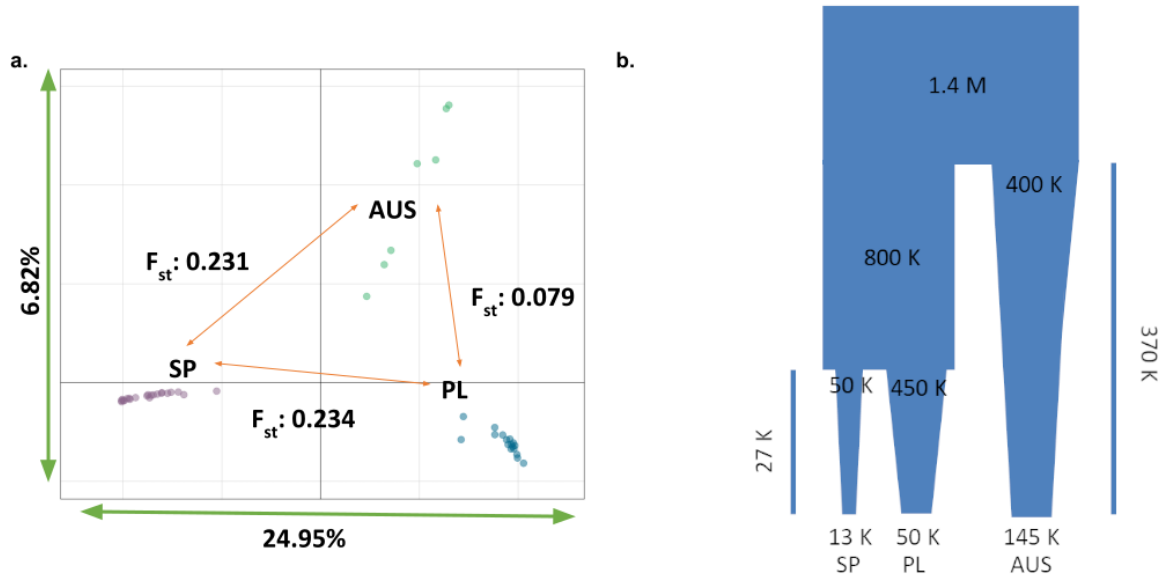

Fig. 1: Population differentiation and demographic analysis of 3 *Arabidopsis lyrata* ssp. *petraea* populations. a. Principal Components analysis of Spiterstulen (SP), Plech (PL) and AUS (Austria) samples. The first Principal Component (PC) explains 24.95% of the sample variation and the second PC explains 6.82%. Within the PCA plot the F_{ST} values between all the population pairs are given. **b.** Schematic representation of the demographic scenario used for parameter estimation. Within the graph the effective population size (Ne) of the ancestral populations before and after the population splits are given. At the bottom of the graph the estimated current Ne for each population is presented, while at the sides the time since the population splits is provided in thousand years.

Estimated effective population sizes before and after divergence events indicated bottlenecks in all populations. The size estimate of the ancestral population reached N_e= 1,423,150 (CI: 749,730 - 1,689,543). The effective population size (N_e) of SP was reduced approximately 34-fold after it diverged from PL, from N_e= 854,105 (CI: 725,852 – 1,035,236) to N_e=24,613.5 (CI: 15,761 – 44,521), respectively before and after the split. In contrast, the PL population experienced a weaker bottleneck to approximately a third of the ancestral size N_e= 854,105 after the split, N_e=444,159.5 (CI: 209,396 – 817,377). The bottleneck in AUS was of the same magnitude with N_e= 398,310(CI: 286,928 – 411,328) after it split from PL and SP. Furthermore, after splitting from each other, all populations shrunk progressively towards the current Ne values, which were estimated to be Ne = 13,652.5 (CI: 6609 – 28,726), Ne=50,610 (CI: 23,949 – 104,827) and Ne=145,770 (CI: 56,938 – 198,579) for SP, PL and AUS respectively. The decline in population size was inferred to be steady, and models with a constant population size were rejected. We note, however, that the AUS sample consists of individuals collected from three closely located sites, and thus might reflect diversity at a coarser grain than the SP and PL samples.

To test the robustness of bottleneck inference to sample size, we also conducted the demographic modelling with down-sampled data sets (1/3 and 2/3 of SP and PL sample sizes). Even though down-sampling decreased the N_e estimates, the fold reductions and differences between the populations remained comparable (Table S4). The demographic modeling therefore confirmed that PL, AUS and SP are clear, contrasting range-core and-edge populations (Muller et al. 2008; Pyhäjärvi et al. 2012; Mattila et al. 2017). This supports a scenario of colonization in Scandinavia with genetic material from Central European glacial refugia, a history that is common to several plant species (Clauss and Mitchell-Olds 2006; Ross-Ibarra et al. 2008; Ansell et al. 2010; Schmickl et al. 2010; Pyhäjärvi et al. 2012, Laenen et al. 2018; Pyhäjärvi et al. 2007).

We calculated Tajima's D values in 10kb windows for each population (Fig 2a). The distribution of Tajima's D values for SP was shifted towards positive values (mean = 1.230, median = 1.286), which was consistent with the inferred demographic history of a strong recent bottleneck in SP. Tajima's D values for PL and AUS were also mainly positive (mean = 0.313, median 0.265 for PL and mean =0.240, median =0.151 for AUS) but both were significantly lower than in SP (Kolmogorov-Smirnov, KS test p-val < 2.2e-16 in both cases). The two populations' distributions also differed significantly (KS test p-val < 2.2e-16).

Additionally, analysis of linkage disequilibrium (LD) decay further confirmed the stronger bottleneck experienced by the SP population. LD decay was calculated on the subsample of 12 field collected SP individuals to ensure that native LD levels were analyzed (Individuals obtained from crosses in the greenhouse were removed). LD was halved within 2.2 kb in SP, which is considerably slower than for an equally sized sample of PL individuals (LD halved within 0.5kb; Fig. 2b).

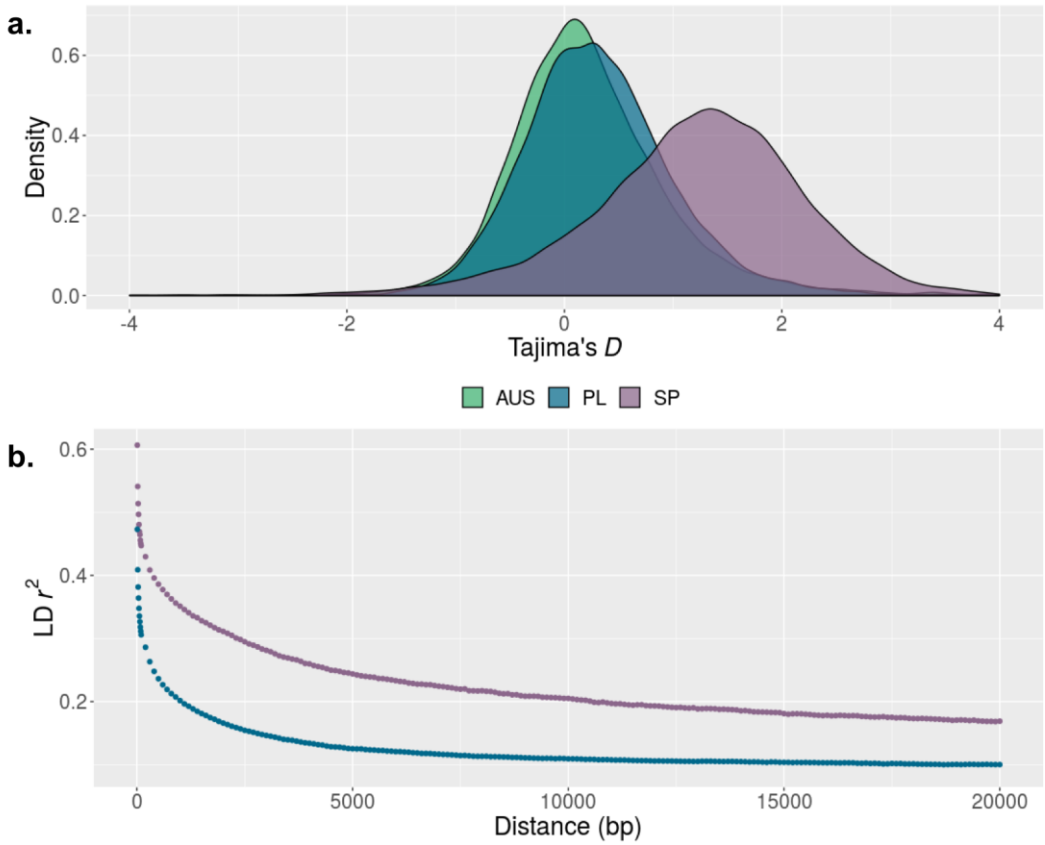

Fig. 2: Evidence of a strong bottleneck along the SP genome. a. Tajima's D distribution for AUS, PL and SP calculated along the chromosomes in 10kb non-overlapping windows. The density is calculated so that the total area bellow the curve is equal to 1. **b.** Linkage decay for SP and PL as a function of SNP pairwise r^2 and the distance between the SNPs. The sample size of the two populations was equal, with 12 individuals each.

To give insight into how the effective population size of *A. l. ssp. petraea* compares to *A. l. ssp. lyrata*, we computed the population proportion of derived non-synonymous mutation, which was used as an indicator of the efficacy of selection and therefore the effective population size (N_e) in *A. l. ssp. lyrata* pool sequencing data (Willi et al. 2018). This statistic was slightly higher in SP (0.5338) than in PL (0.5298) and much lower than reported even for outcrossing populations of the mixed-mating relative *A. l.* ssp. *lyrata* (0.75-1, Sup Table 3, Willi et al. 2018). This indicates that, in comparison with *A. l.* ssp. *lyrata*, the effective population size of *A. l.* ssp. *petraea* is higher throughout its range.

The distribution of fitness effects

To infer the efficiency of negative selection, we estimated the distribution of fitness effects in both core (PL) - and range-edge (SP) populations (Fig 3a and 3b). As the AUS population had a smaller

sample size, as well as individuals taken from three different local sites, it was excluded from the estimation of the distribution of fitness effects of new variants (DFE). The distributions of the full spectrum of fitness effects (DFE) was estimated by contrasting the synonymous (4-fold) and nonsynonymous (0-fold) unfolded SFS using the software polyDFEv2.0 (Tataru and Bataillon, 2019). A likelihood ratio test comparing the fit of model where DFE parameters were estimated independently for the two populations to a model where they were estimated jointly rejected a single distribution of the product Ne*s for both SP and PL (p-value = 1.425219e-41; Fig S3). In PL, the proportion of new variants inferred to be nearly neutral ($-1 < Ne*s < 0$) reached 0.18, with the majority (60%) of variants being highly deleterious ($Ne*s > -10$) (Fig 3b). A small but significant proportion of mutations were predicted to be adaptive, forming a fraction of 10^{-6} of all variants (Fig 3b). A distinct DFE was inferred in SP (Fig. 3b). How the two distributions relate to each other, however, is difficult to interpret. Indeed, most variants are shared between SP and PL (Fig. 3a), and the elevated Tajima's D in SP indicates that the population has not yet returned to equilibrium, rendering the comparison of inferred $N_{e*}s$ difficult (Fig 2a). It however shows that non-synonymous variants segregate at higher frequency in the SP populations and gives an acceptable estimate of the proportion of slightly deleterious mutations that may evolve under relaxed selection in SP (Fig 3a).

Measures of accumulated burden in SP individuals

The number of derived non synonymous mutations per Mbp of each lineage has been shown to be an appropriate proxy for genomic burden, because its expectation is unaffected by demographic events (Simons and Sella 2016). The demographic model and DFE inferred in PL provided useful parameters to quantify the maximum burden we can expect to find in SP, if selection on slightly deleterious mutations had been completely relaxed after the bottleneck. We assumed a mutation rate of 7.10^{-9} mutations per generation per nucleotide (Ossowski et al. 2010), we multiplied this rate by the predicted time since the split between SP and PL, and by the total number of non-synonymous sites in the genome to have a total of $2*7.10^{-9}*2.10^{7}*26{,}902\sim=7{,}500$ expected non synonymous mutations per diploid genome. Assuming, as indicated by the DFE in PL that 60% of new mutations are strongly deleterious so that individuals carrying them were removed from the population, we expect about 3,000 neutral or nearly neutral mutations accumulated in the genome of SP individuals since the split from PL.

Evaluating the cumulative fitness impact of these mutations requires estimates of s. If these mutations follow the distribution of fitness effects inferred in PL, whose ancestral population size N_e approaches 1M; we roughly predict that each of these mutations will have an s ranging from 0 to -10^{-5} ($-10<N_e.s<0$). If their individual fitness is multiplicative, they will at most contribute a loss of 3% in relative fitness ($10^{-5}*3.000$). This loss in fitness through fixation of nearly neutral mutations in the range-edge population is of the order of magnitude of the one predicted in simulations (Gilbert et al.

2017). We acknowledge that this is a crude extrapolation in the absence of a direct estimation of the distribution of s. However, we believe this calculation is useful in providing a sense of the upper bound on the magnitude of the expansion load that accumulated in SP compared to PL.

This estimate approaches observations of individual burden accumulated in the range-edge population. We measured the accumulated burden of deleterious mutations per individual haploid genome in SP and PL by calculating the mean number of derived mutations per haploid genome and corrected by the total number of genotyped sites genome wide (see Methods). As expected, the mean number of derived synonymous mutations did not differ between the populations (Fig S4). For each sample, we further estimated the mean number of derived non-synonymous mutations (Fig 3c). The average burden accumulated by SP individuals reached a mean 0.0123 non-synonymous mutation per site genome wide (CI: 0.0118 – 0.0127). For PL the mean burden was 0.0117 (CI: 0.0113 – 0.0121). We detected, on average, an excess of 12,000 derived non-synonymous mutations per haploid genome in SP individuals, compared to PL. This number was of the same order of magnitude as the expected number of mutations we extrapolated from population genomics parameters (3,000). Nevertheless, after bootstrapping across 1Mbp genomic blocks, populations did not show a significant difference in mean accumulated burden (p-val = 0.51 for SP vs PL). Even individuals of the AUS population, with its larger population size, did not show a significantly lower burden of non-synonymous mutations (AUS, 0.0104 non-synonymous mutation per site, CI: 0.0100 – 0.0108, p-val = 0.5 for SP vs AUS and p-val=0.491 for PL vs AUS). There was a small shift towards a smaller average number of non-synonymous mutations per genome in AUS, but since this shift was also observed for the same number of synonymous mutations, it likely reflects the lower average genomic coverage of AUS whole genome sequences.

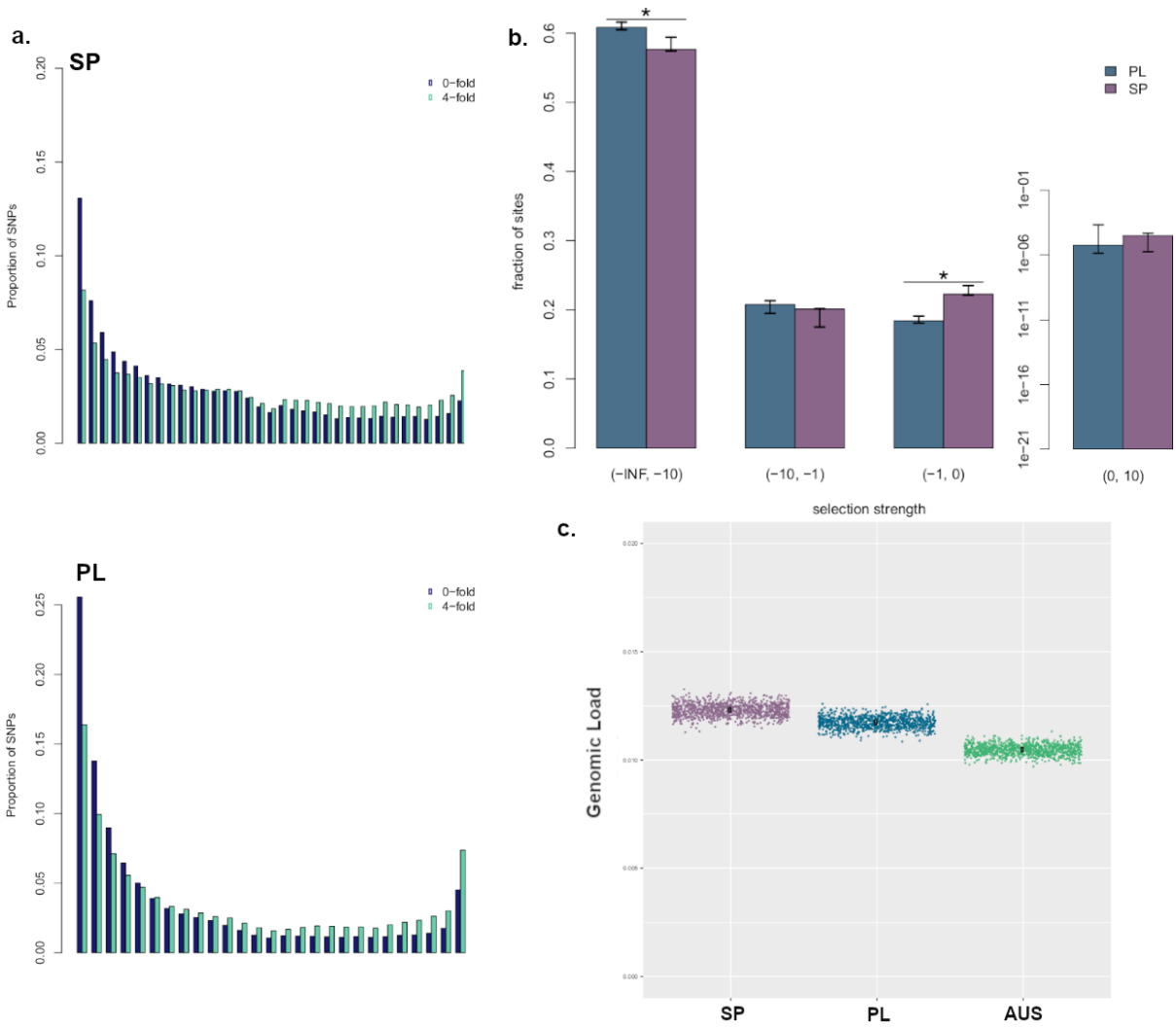

Fig. 3: Effectiveness of selection and genomic load per population. a. Unfolded site frequency spectrum for SP (top) and PL (bottom) populations. **b.** Estimated discretized distribution of fitness effects (DFE) is shown for the two *A. lyrata* populations PL and SP. Whiskers show the 95% confidence intervals for each bin. The strength of selection is given as the effective population size times the selection coefficient (N_e*s). **c.** Genomic load for each population calculated as the number of non-synonymous corrected by the total number of genotyped sites per sample. For each population, the population mean obtained by each bootstrap is shown in color and the original mean is also marked with black dots. For AUS, not only the total number of non-synonymous sites is lower but also the synonymous sites are less (see als o Fig S4). This is probably the result of lower genome coverage of the population, which led to not lower estimate.

SP and PL show similar growth rate in a common garden of the species in the range core.

We further investigated whether individuals in the SP population show a decrease in individual growth rate. We planted six replicate cuttings of 10 genotypes of each of the two population in the

common garden of University of Cologne. The experiment was initiated early autumn and terminated a year later at the end of the growth season. Although individuals of SP had a comparatively lower rosette area after winter, the rosette area (p-val = 0.265) as well as their accumulated biomass (p-val=0.2873) did not differ from that of PL individuals at the end of the growth season (Fig S5), due to different growth over time of the two populations (Month and Population interaction p-val < 2.2e-16). This is in agreement with previous reciprocal transplant experiments (Leinonen et al. 2009).

Selective sweeps in the range edge are broader than in the core but equally frequent

We searched for the footprints of selective sweeps within SP and PL – the two populations with the largest sample sizes using the Composite Likelihood Ratio (CLR). CLR estimates were computed in windows along the chromosomes with *SweeD* (Pavlidis et al. 2013). Significant deviations from neutral expectation were defined by comparing the observed diversity estimates to neutral diversity estimates simulated under the demographic model obtained above. We used the overlap of outlier CLR and F_{ST} to identify putative selective sweep regions specific to SP or PL (and thus indicative of local selection). We detected signatures of local sweeps within both populations despite their large differences in recent effective population size. In SP, we identified 1620 local sweep windows, which grouped in 327 genomic regions of average size 7051bp (see methods). Within PL, 745 windows, covering 104 genomic regions (average size 4384bp), had PL specific signatures for sweep.

Genes within the genomic regions carrying a population-specific signature of a selective sweep were extracted and tested for functional enrichment (Supplementary Information). In SP, fifteen Gene Ontology (GO) terms were enriched among genes showing signatures of positive selection (significance based on permutation derived p-val threshold of 0.0295). The top three GO terms were “cellular response to iron ion”, “response to mechanical stimulus” and “response to hormone”. In PL, three GO enriched terms were significant (p-val threshold of 0.02137) and they were “intra-Golgi vesicle-mediated transport”, “regulation of anion transport” and “monosaccharide metabolic process” (Table S5).

We further investigated whether specific candidate gene groups carried signatures of adaptive evolution. First, we searched for functional enrichments among the most differentiated genes. An excess of high F_{ST} values was detected for genes involved in development (p-val = 0.0183) and light (p-val = 0.0364). Second, we explored whether specific groups of genes associated with traits known or likely to be locally adaptive, carried signatures of adaptive evolution. Phenotypic differences in flowering time and especially selection related to the photoperiodic pathway, or to development have been shown to contribute to local adaptation in SP (Toivainen et al. 2014; Mattila et al. 2016; Hämälä and Savolainen, 2019), and response to abiotic factors such as cold and drought (Vergeer and Kunin 2013; Davey et al. 2018). We used the *A. thaliana* annotation to identify genes involved in the regulation of the previous phenotypes. We then tested whether their F_{ST} estimates tended to be higher than the rest

of the annotated genes (Table S6). We detected a significant excess of high F_{ST} values for genes involved in development (KS test Bonferroni corrected p-val = 0.0183) and genes annotated for a role in the plant response to light (KS test Bonferroni corrected p-val = 0.0364).

Negative frequency-dependent selection maintained S-locus diversity in the range-edge population

Despite a smaller effective population size in SP, strong negative frequency-dependent selection acting on the self-incompatibility locus effectively maintained or restored S-allele diversity. In SP, 15 S-alleles (allelic richness was equal to 7.6) were detected across 22 individuals, with gene diversity at the S-locus equal to 0.828. Within the 18 PL individuals, 14 S-alleles (allelic richness = 8.1) were found (gene diversity = 0.877) and 10 S-alleles (allelic richness = 10.0) were observed among the 7 AUS individuals (gene diversity = 0.940) (Table 1; Table S7). High S-allele diversity in SP, together with absence of evidence of excess of homozygosity at control loci (see below), suggests that individuals are highly outcrossing and thus that the past bottleneck does not seem to have affected the mating system. The S-locus F_{ST} between SP and either PL or AUS was equal to 0.027 or 0.037, respectively, values much lower than the whole genome (0.231 or 0.234, respectively) as predicted by Schierup et al. (2000).

Table 1: S –locus allelic diversity has been maintained within SP. The number of S-alleles for each population sample, as well as the number of individuals is provided. For each population the allelic richness has been calculated according to a rarefaction protocol with *N*=7.

Population	**S - alleles**	**Allelic Richness**	**Sample Size**
SP	15	7.6	22
PL	14	8.1	17
AUS	10	10.0	7

To further test whether self-incompatibility was effectively enforced in the Northern population, we analyzed the genotypic composition of these populations. Inbreeding or cryptic population structure is expected to create an excess of homozygous genotypes, compared to the Hardy-Weinberg expectation in a random mating population. The relatively large number of sampled individuals within SP and PL allowed the examination of the relative excess or deficit of homozygous genotypes. Positive F_{IS} values indicate an excess of homozygous genotypes and negative values an excess of heterozygous geno-

types. As expected for an obligate outcrossing species, the F_{IS} distribution was approximately centered on 0 in PL (mean = -0.0447, median = -0.013). We excluded individuals amplified in the greenhouse from the analysis. If the presence of cryptic selfing had increased inbreeding in SP, we would expect a shift of the F_{IS} distribution towards positive values. This was not the case: the F_{IS} distribution offield collected SP individuals (see methods), was not shifted towards positive values (mean = -0.1323, median = -0.321). The genome wide analysis of inbreeding coefficients F_{IS} thus confirmed that obligate outcrossing is effectively maintained in the Northern population. We detected however a significant difference of the F_{IS} distribution of the two populations, indicating a greater number of loci in SP with an excess of heterozygotes (Fig S6, KS test p-val < 2.2e-16). We found no indication that the F_{IS} values result from artefacts such as imperfect genome assembly or variation in copy number (Suppl. Document). Larger samples sizes will be needed to assess the excess of heterozygotes with greater accuracy.

Discussion

No detectable genomic burden in the SP range-edge population

The relationship between population size and selection is a centerpiece of population genetics theory. At equilibrium, smaller populations have a lower adaptive potential and increased burden of deleterious alleles. These premises formed a viewpoint that population bottlenecks reduce the removal of deleterious mutations (Hamilton 2009). In reality however, it takes time until the equilibrium between gain and loss of mutations is restored in a bottlenecked population, so that population size reduction does not immediately associate with the presence of an increased mutation burden.

The SP population provides a clear case of a range-edge population likely exposed to successive severe bottlenecks but with only a mild increase in average burden of deleterious mutations. Demographic modeling estimated that the population progressively decreased to about 3% of its initial size. In agreement with previous reports (Mattila et al. 2017; Hämälä et al. 2018), this decrease had pronounced population genetics consequences: a markedly lower level of diversity, a slower LD decay and non synonymous variants segregating at higher frequency. The genome-wide elevation of Tajima's *D* further indicates that the population has not yet returned to equilibrium, since it is still depleted in rare alleles relative to common ones. Simulations showed that a short term bottleneck produces hardly any effect on haploid number of deleterious alleles per individual (Do et al. 2015, Simons and Sella 2015). In modern human populations, the per-individual burden of deleterious alleles in range-edge populations is not distinguishable from range core populations, despite a documented excess of common non synonymous alleles (Do et al. 2015). Likewise, the expected increase in burden in SP, assuming that selection is entirely relaxed, is too small to be detected given both experimental uncertainties and heterogeneity along the genome, even if the population bottleneck experienced by SP is longer in time. In addition, the number of potentially deleterious mutations that have accumulated in

individual genomes after the bottleneck is very small in contrast to the total burden individual genomes are likely to have accumulated. Further, the measure we took does not account for recessive deleterious alleles, but since these have been predicted to be enriched among strongly deleterious mutations in *A. lyrata* (Huber et al. 2018), they are unlikely to increase the difference in average per individual burden we report here for edge- vs core-range populations.

Assuming that post-glacial re-colonization occurred approximately 26,000 years ago, as estimated in this study, our calculation that at most 7,000 new non-synonymous mutations have occurred in each individual genome sets an upper limit on the maximum load that a decrease in population size can ever cause to accumulate after the last glaciation. In other words, the maximum expansion load cannot be greater than what a mutation accumulation line would have accumulated if it had been selfed for 26,000 generations (Ossowski et al. 2010; Do et al. 2015). The severity and duration of the bottleneck will only influence the fraction of these new deleterious mutations that are not removed by selection and accumulate within genotypes. Significant mutation load has neverthelesss been associated to post-glacial expansion in several instances, where the expansion bottleneck was more severe because of a shift in mating system. Individuals of the sister sub-species *A. l. ssp. lyrata* showed a marked increase in phenotypic load at the range edge, particularly in populations that shifted to selfing (Willi et al. 2018). In *Arabis alpina*, individuals sampled in a selfing population of the species Northern European range also appeared to have accumulated a greater load of deleterious mutations than other populations closer to the range-core (Laenen et al. 2018). The metric we used for the genomic burden has the considerable advantage that it is insensitive to variation in population size, but it remains a crude estimator. Indirect methods may be more powerful. For example, patterns of Neanderthal introgression in the modern human genome, revealed the increased deleterious load of the introgressing genome (Juric et al. 2016). In maize, an outcrossing crop, which experienced two successive drastic bottlenecks during domestication, it is the variance in gene expression that revealed the existence of a burden of deleterious regulatory mutations that significantly impaired fitness (Kremling et al. 2018). In *A. l. ssp. petraea*, however, the lack of fitness difference observed in common garden within the range-core area provides a strong indication that SP individuals do not suffer from a strong deleterious burden (Fig. S5, Leinonen et al. 2009).

Evidence for effective negative-frequency dependent selection

Small size populations are also expected to require larger effect mutations to respond to selection (Hamilton 2009). This, however, does not impair the response to negative frequency-dependent selection on S-allele, and the maintenance of an effective level of outcrossing. The S-locus diversity, both in terms of allelic richness and heterozygosity, was found to be only marginally lower in SP compared to PL and AUS. The presence of several S-alleles was also reported for 12 Icelandic *A. lyrata* ssp *petraea* populations (Schierup et al. 2008), that share recent history with SP (Pyhäjärvi et al. 2012).

This, together with the observation that homozygote genotypes (and thus crypting selfing events) are not more frequent throughout the genome, confirms that SP has maintained a functional self-incompatibility system, despite the historical genetic bottleneck. The persistence of obligate outcrossing in Scandinavian *A. l.* ssp. *petraea* populations has previously been discussed by Sletvold et al. (2013), who attributed the maintenance of a functional self-incompatibility system to the strong inbreeding depression levels occurring in those populations. In contrast, low inbreeding depression in North American populations of *A. lyrata* ssp. *lyrata* may have been a key feature that contributed to independent breakdown of self-incompatibility associated with bottlenecks at the species distribution edges (Willi et al. 2013; Willi et al. 2018). Comparable to the North American populations of *A.l. ssp lyrata*, many other examples of loss of self-incompatibility have been reported after range expansion or strong genetic bottlenecks. For example, Scandinavian populations of *Arabis alpina* (Laenen et al. 2018), disjunct marginal populations of race a4 in *Leavenworthia alabamica* (Busch et al. 2011), and strong bottleneck associated with loss of self-incompatibility and speciation in *Capsella rubella* (Guo et al. 2009). Our result also illustrates the remarkable power of negative frequency-dependent selection acting on the S-locus at promoting a high level of resilience against the effect of a bottleneck on allelic diversity. Similar results were found in *Leavenworthia alabamica,* were the authors did not find reduced S-allele diversity or mate limitation in outcrossing populations from small patches as compared to large populations (Busch 2005). Even if allelic diversity could have been reduced at the time of bottleneck in Scandinavian populations of *A. lyrata*, theory predicts that negative frequency-dependent selection promotes higher effective migration rates at the S-locus as compared to control loci (Schierup 1998), suggesting that high allelic diversity could have been restored subsequently by gene flow.

Adaptive dynamics maintained in SP

Small size populations are also expected to require larger effect mutations to adapt, although these mutations are rare (Hamilton 2009). Whether a population size reduction immediately reduces adaptive evolution is, however, a complex question in the context of range expansion (Gilbert et al. 2017). If populations have to adapt locally at the range edge, the rate of geographical expansion slows down, along with the severity of the expansion bottleneck (Gilbert et al. 2017). A decrease in population size, however, increases the range of beneficial alleles that behave effectively neutrally (Lynch 2007). Searching for signals of selective sweeps in SP, after accounting for its demography, we identified 327 regions that formed outlier for both CLR and F_{ST} statistics. In fact, the number of genomic regions displaying a signature of positive selection was greater in SP than in PL, a pattern that has been observed also in Northern Swedish populations of *A. thaliana* in contrast to Southern Swedish populations (Huber et al. 2014). However, some of the signal detected in SP could also result from the surfing of new alleles in the range margin, which can mimic signatures of adaptive evolution (Excoffier et al. 2009). To test whether the signals of adaptation were confounded by the surfing of neutral or dele-

terious alleles, we searched for functional enrichments among regions displaying signatures of local positive selection. Within those regions, functions involved in the response to stress were enriched, in agreement with a previous study investigating micro-geographical patterns of local adaptation in Norwegian populations connected by gene flow (Hämälä et al. 2018; Hämälä and Savolainen 2019). We also found a significant enrichment in genes involved in light perception, a function enriched in loci differentiating the SP population from a close-by population of lower elevation (Hämälä and Savolainen 2019c). Furthermore, the F_{ST} distribution of genes related to development was significantly shifted towards higher values, suggesting polygenic selection on alleles associated to this function (Foll et al. 2014; Daub et al. 2015; Stephan 2016). Previous work has documented that Scandinavian populations display differences in several traits related to growth and resource allocation, including plant size, inflorescence production and fruit production (Quilot-Turion et al. 2013; Hämälä et al. 2018). In addition, both local and regional reciprocal transplant experiments have revealed local adaptation, indicating that adaptive dynamics are ongoing also at smaller geographical scale (Leinonen et al. 2009; Hämälä et al. 2018).

Signatures of positive selection in the genome of SP indicate that it has a history of adaptive evolution that is comparable to that observed in PL. Simulations and analytical models of range expansion in strictly outcrossing populations predict fewer large effect adaptive mutations and an increased proportion of mutations with a small positive effect on fitness in range-front populations (Peischl et al. 2015). The maintenance of strict outcrossing in *A. l. ssp. petraea,* which was possibly favored by the maintenance in S-allele diversity we document, probably contributed to milden the decrease in effective population size and sustain adaptive evolution(Charlesworth Deborah et al. 1979). In contrast to selfing populations, strictly outcrossing populations should indeed be able to more effectively decouple adaptive mutations from the background in which they arise. This process helps mitigate the accumulation of an expansion load, but it also prevents the occasional invasion of range margin populations with exceptionally high-fitness lineages (Peischl et al. 2015). The predicted proportion of mutations with a large or small beneficial effect on fitness was not significantly different in the two populations, a finding which, here again has to be taken with caution given that the population is not at equilibrium. Our analyses nevertheless show that range expansion in the European *A. l. ssp. petraea* associates with a decrease in population size but did not alter adaptive dynamics, presumably thanks to the maintenance of both outcrossing and gene flow (Gilbert et al. 2017; Hämälä and Savolainen 2019).

Materials and Methods

Plant Material, Sequencing and Data Preparation

Genomic sequences of *A. l. ssp. petraea* populations of 22 individuals originating from Spiterstulen in Norway (SP; 61.41N, 8.25E), 17 individuals originating from Plech in Germany (PL; 49.65N,

11.45E) and a scattered sample of 7 individuals from Austria (AUS; 47.54N, 15.58E; 47.55N, 15.59E; 47.58N, 16.9E) were used in the analysis (Fig S1). Details on the sequencing methodology is given in Supplementary Information.

Analysis of population structure

Genetic diversity and differentiation along the chromosomes were calculated with PopGenome package (Pfeifer et al. 2014) in the R environment version 3.4.4 (R Core Team 2018). Specifically, we calculated pairwise nucleotide fixation index (F_{ST}), nucleotide diversity between (d_{xy}) and within population (π) in 10kb non overlapping windows for each chromosome with functions F_ST.stats, diversity.stats.between and diversity.stats.within, respectively (Wakeley 1996; Hudson and Wayne, 1992). In order to avoid biased F_{ST} estimates (Cruickshank and Hahn 2014), the windows that had F_{ST} above 0.8, dxy and π below 0.001 in at least one population comparison, were removed from the analysis. Tajima's D was calculated with the function neutrality.stats of PopGenome. The Linkage Desequilibrium for the field collected SP and PL individuals was calculated along the genome with the default functions of PopLDdecay (Zhang et al. 2019) and the values were plotted in R.

Principal component analysis (PCA) of the genomic data was conducted with adegenet package (Jombart 2008) using a file we had retained every 300th SNP to reduce computational load. This reduced dataset of 233075 SNPs was used to calculate SNP based F_{IS} for each population with Hierfstat (Goudet 2005) package function basic.stats (Alexander et al. 2009; Goudet and Jombart 2015). The F_{IS} value of each gene was estimated based on the median F_{IS} value of its SNPs, for SP and PL.

For the admixture analysis (Alexander et al. 2009) bed files were generated with PLINK (Purcell et al. 2007), which were then analyzed for clusters K=1 till K=5, with 10 iterations of cross-validation each. The clusters were normalized across runs using CLUMPAK (Kopelman et al. 2015) and subsequently they were plotted in R.

Demography simulations

To study the demographic history of these populations, we conducted site frequency spectra (SFS) based coalescent simulations with fastsimcoal2 v2.6.0.3 (Excoffier et al. 2013). Folded 3D SFS, comprising of SP, PL and AUS individuals, was estimated from 4-fold sites with ANGSD v0.917 (Korneliussen et al. 2014), using the same filtering steps as with variant calls. Models with different divergence orders and migration scenarios were repeater 50 times and ones with highest likelihoods were retained. Model selection was based on Akaike information criterion (AIC) scores. Confidence intervals were estimated by fitting the supported model to 100 nonparametric bootstrap SFS. We used these models to define effective populations sizes (N_e), divergence times (T) and migration rates (m). To evaluate how the estimated demography influences measures of positive selection, we used the N_e,

T and *m* parameters in combination with recombination rate estimates derived from an *A. lyrata* linkage map (Hämälä et al. 2017) to generate 10,000 10 kb fragments with *ms* (Hudson 2002). These data were then used to define neutral expectations for analysis of positive selection.

polyDFE

For analyzing the strength of selection, vcf files were first re-filtered for each population separately, as described in the section "data preparation". This was done to retain positions that only needed to be removed in one population. Sites were further downsampled to have the same number of observed alleles in all populations. Ancestry information was based on a whole genome alignment of *A. lyrata* v1, *A. thaliana* TAIR10 (Lamesch et al. 2012), *A. halleri* v1 (DOE-JGI, http://phytozome.jgi.doe.gov/) and *C. rubella* v1 (Slotte et al. 2013), and an unfolded frequency spectrum was determined for each species (Fig. 3).. Details on the pipeline are given in Supplementary Information. To establish the distribution of fitness effects, we tested whether the DFE parameters were shared or different between the populations. For this, we first ran polyDFEv2 (Tataru and Bataillon, 2019) under standard settings and using the –w flag to exclude the divergence data and calculated the DFE parameters either independently or shared between the populations. Models were compared using the likelihood ratio test (LRT). 200 bootstrap SFS were then generated using the bootstrapData function in the processing R script of polyDFEv2. These replicates were run for SP and PL using the independent parameters estimated for the DFE as starting values (Table S10) for local optimization.

Genomic burden estimates and comparison with *A. l. ssp. lyrata*

We used the number of derived non-synonymous mutations per individual to quantify the population's genomic burden (Simons and Sella, 2016). We used SNPeff (Cingolani et al. 2012) to annotate synonymous and non-synonymous sites, whose ancestral state was inferred in the polyDFE pipeline described above. Then we counted their respective numbers per individual, with weight of +1 for each instant of homozygous state of the derived allele and as +0.5 for the heterozygous sites. We divided the counts by the total number of genotyped sites, in order to correct for differences in genome mapping between the individuals. The genomic load of each population was calculated as the mean of the non-synonymous sites of individual samples, while the synonymous sites were used to confirm the robustness of the analysis, as they are expected to be not different among the populations. The confidence intervals for each population, as well as the p-values for the pairwise population comparisons, were estimated by bootstrapping 1Mbp windows to simulate each time a whole genome (207 1Mb regions) and extracting the population means in each bootstrap round.

To compare the proportion of non-synonymous mutations in the *A. l. ssp. petraea* populations to the *A. l. ssp lyrata* populations, which had been pool-sequenced, we computed the population average proportion of non-synonymous mutations as in Willi et al. (2018). This measure was shown to scale

with phenotypic measures of mutation load in *A. l. ssp. lyrata* (Willi et al. 2018), but it cannot be used for comparison across species, because it is sensitive to demographic parameters (Simons & Sella, 2016).

Comparative analysis of growth rate and biomass accumulation in a common garden experiment

We propagated clonally 10 genotypes from SP and 10 from PL to study growth in a common garden setting. The experiment was initiated in September 2017 and ended August 2018 and took place at the common garden of the University of Cologne. Throughout the growing season (March to August) we scored monthly diameter size, in millimeters, as a proxy for vegetative growth. At the end of the growing season, we harvested the above ground material to estimate the dry to fresh weight ratio of the plants as a proxy for the plants' biomass. Differences between the two populations were tested in R with linear mixed models using the library lme4 (Bates et al. 2015). The model included population and month of the measurement taken as fixed effects. The genotype and replicate number were included as random effects in order to correct for pseudoreplication resulting from measuring every time the same plants. Significance levels were estimated with the function Anova, from car library (Fox and Weisberg 2019).

Scan for selective sweeps

Areas influenced by selective sweeps were inferred by estimating composite likelihood ratios with SweeD v4.0 (Pavlidis et al. 2013). The analysis was done in 2 kb grid sizes for the SP and PL samples. As a bottleneck can easily bias CLR estimates (Jensen et al. 2007), we used data simulated under the best supported demographic model to define limits to neutral variation among the observed estimates. Estimates exceeding the 99th percentile of neutral CLR values were considered putatively adaptive. We combined significant grid points within 10 kb regions to create outlier windows. Grid points that had no other outliers within 10 kb distance were removed from the analysis. Next, we examined the sweep regions in combination with regions showing elevated differentiation to find areas targeted by strong selection after the populations diverged. As with CLR, windows with F_{ST} values above the 99th percentile of their distribution were considered outliers. Genes from the regions showing higher than neutral differentiation with both CLR and F_{ST} were extracted.

Identification of S alleles

We genotyped individuals at the self-incompatibility locus (S-locus) with a genotyping pipeline (Genete et al. in preparation) using raw Illumina reads from each individual and a database of all available sequences of *SRK* (the self-incompatibility gene expressed in the pistil) from *A. lyrata*, *A. halleri* and *Capsella grandiflora* (source: GenBank and unpublished sequences). Briefly, this pipeline

uses Bowtie2 to align raw reads against each reference sequence from the database and produces summary statistics with Samtools (v1.4) allowing to identify alleles at the S-locus (S-alleles). Coverage statistics allow to reliably identify homozygote versus heterozygote individuals at the S-locus. Genotype data was used to compute population genetic statistics using Fstat (Goudet 1995): number of alleles per sample, sample allelic richness (a standardized estimate of the number of alleles taking into account differences in sample sizes among populations, computed after the rarefaction method described in El Mousadik and Petit 1996), gene diversity (expected heterozygosity under Hardy-Weinberg hypotheses), and F_{ST} (unbiased estimate of the among population fixation index).

Identification of gene functional groups and functional enrichment analysis

F_{ST}, dxy and π were estimated for all genes according to the *A. lyrata* gene annotation version 1.0.37 with PopGenome and as described above for the genomic windows. We extracted the genes and their corresponding statistics F_{ST} and CLR statistics. Genes that had functions involved in light, cold, flowering, plant development and dormancy were determined based on the gene ontology of the sister species *A. thaliana*. To explore whether the aforementioned groups of genes had genetic differentiation estimates that were significantly different from the genome-wide background, we performed a non-parametric, two sample Kolmogorov Smirnov test (Marsaglia et al. 2003) between the gene group of interest and the rest of the genomic genes identified in *A. thaliana* and belong in a GO group (ks.test function in R).

We ranked the genes by descending order based on their F_{ST} values and run the GO test, using the ks statistic test to evaluate the enrichment with the topGO package (Subramanian et al. 2005; Alexa and Rahnenfuhrer 2016). We permuted the F_{ST} values of the genes 1000 times to obtain a p value cut off at 0.0179 to maintain false discovery rate below 5%. The GO enrichment analysis was done separately for genes located in candidate sweep regions, and for genes located in both candidate sweep and F_{ST} (SP vs PL) outlier regions. Significance of the enrichment was evaluated with Fisher's exact test.

Data Availability

All sequence data are available in either NCBI Short Read Archive (SRA; https://www.ncbi.nlm.nih.gov/sra) or in the European Nucleotide Archive (ENA; https://www.ebi.ac.uk/ena) with accession codes: SAMN06141173-SAMN06141198 (SRA; Mattila et al. 2017), SRP144592 (SRA; Hämälä et al. 2018), PRJNAXXXXX (ENA; Marburger et al. 2019), and PRJNAXXXXX (ENA; whole genome sequences generated for this project and the rest of PL sequences).

Acknowledgements

We thank M. Nothnagel, B. Wieters, and G. Schmitz for insightful discussions and comments on the results; M.Nordborg and P.Novikova for PL sequences; B. Laenen and Viera Kovacova for help with the polyDFE data preparation; K. Bell for lab assistance; students at the university of Cologne for assisting with the field experiment; and Cologne Center for Genomics (Now West Germany Center) for sequencing of SP samples. This project was funded by ERC project 648617 Adaptoscope.

References

Alexa A, Rahnenfuhrer J. 2016. topGO: Enrichment Analysis for Gene Ontology. R package version 2.30.1.

Alexander DH, Novembre J, Lange K. 2009. Fast model-based estimation of ancestry in unrelated individuals. Genome Res. 19:1655–1664.

Austerlitz F, Jung-Muller B, Godelle B, Gouyon P-H. 1997. Evolution of Coalescence Times, Genetic Diversity and Structure during Colonization.

Baker HG. 1995. Self-Compatibility and Establishment After “Long-Distance” Dispersal. 9:347–349.

Barrett SCH. 2003. Mating strategies in flowering plants: the outcrossing–selfing paradigm and beyond.Dickinson HG, Hiscock SJ, Crane PR, editors. Philosophical Transactions of the Royal Society of London. Series B: Biological Sciences 358:991–1004.

Bateman AJ. 1955. Self-incompatibility systems in angiosperms: III. Cruciferae. Heredity 9:53–68.

Bates D, Mächler M, Bolker B, Walker S. 2015. Fitting Linear Mixed-Effects Models Using lme4. Journal of Statistical Software 67:1–48.

Busch JW. 2005. The evolution of self-compatibility in geographically peripheral populations of Leavenworthia alabamica (Brassicaceae). American Journal of Botany 92:1503–1512.

Busch JW, Joly S, Schoen DJ. 2011. Demographic Signatures Accompanying the Evolution of Selfing in Leavenworthia alabamica. Molecular Biology and Evolution 28:1717–1729.

Charlesworth Deborah, Charlesworth Brian, Maynard Smith J., Holliday Robin. 1979. The evolutionary genetics of sexual systems in flowering plants. Proceedings of the Royal Society of London. Series B. Biological Sciences 205:513–530.

Cheptou P-O. 2012. Clarifying Baker’s Law. Ann Bot 109:633–641.

Cingolani P, Platts A, Wang LL, Coon M, Nguyen T, Wang L, Land SJ, Lu X, Ruden DM. 2012. A program for annotating and predicting the effects of single nucleotide polymorphisms, SnpEff. Fly (Austin) 6:80–92.

Clauss MJ, Koch MA. 2006. Poorly known relatives of Arabidopsis thaliana. Trends in Plant Science 11:449–459.

Colautti RI, Barrett SCH. 2013. Rapid Adaptation to Climate Facilitates Range Expansion of an Invasive Plant. Science 342:364–366.

Corre VL, Kremer A. 1998. Cumulative effects of founding events during colonisation on genetic diversity and differentiation in an island and stepping-stone model. Journal of Evolutionary Biology 11:495–512.

Cruickshank TE, Hahn MW. 2014. Reanalysis suggests that genomic islands of speciation are due to reduced diversity, not reduced gene flow. Mol Ecol 23:3133–3157.

Daub JT, Dupanloup I, Robinson-Rechavi M, Excoffier L. 2015. Inference of Evolutionary Forces Acting on Human Biological Pathways. Genome Biology and Evolution 7:1546–1558.

Davey MP, Palmer BG, Armitage E, Vergeer P, Kunin WE, Woodward FI, Quick WP. 2018. Natural variation in tolerance to sub-zero temperatures among populations of Arabidopsis lyrata ssp. petraea. BMC Plant Biology 18:277.

Do R, Balick D, Li H, Adzhubei I, Sunyaev S, Reich D. 2015. No evidence that selection has been less effective at removing deleterious mutations in Europeans than in Africans. Nature Genetics 47:126–131.

Durvasula A, Fulgione A, Gutaker RM, Alacakaptan SI, Flood PJ, Neto C, Tsuchimatsu T, Burbano HA, Picó FX, Alonso-Blanco C, et al. 2017. African genomes illuminate the early history and transition to selfing in Arabidopsis thaliana. PNAS 114:5213–5218.

Dwyer KG, Balent MA, Nasrallah JB, Nasrallah ME. 1991. DNA sequences of self-incompatibility genes from Brassica campestris and B. oleracea: polymorphism predating speciation. Plant Mol Biol 16:481–486.

El Mousadik A, Petit RJ. 1996. High level of genetic differentiation for allelic richness among populations of the argan tree [Argania spinosa (L.) Skeels] endemic to Morocco. Theoret. Appl. Genetics 92:832–839.

Excoffier L, Dupanloup I, Huerta-Sánchez E, Sousa VC, Foll M. 2013. Robust Demographic Inference from Genomic and SNP Data.Akey JM, editor. PLoS Genet 9:e1003905.

Excoffier L, Foll M, Petit RJ. 2009. Genetic Consequences of Range Expansions. Annual Review of Ecology, Evolution, and Systematics 40:481–501.

Foll M, Gaggiotti OE, Daub JT, Vatsiou A, Excoffier L. 2014. Widespread Signals of Convergent Adaptation to High Altitude in Asia and America. The American Journal of Human Genetics 95:394–407.

Fox J, Weisberg S. 2019. An R Companion to Applied Regression. Third. Sage Available from: https://socialsciences.mcmaster.ca/jfox/Books/Companion/

Gascoigne J, Berec L, Gregory S, Courchamp F. 2009. Dangerously few liaisons: a review of mate-finding Allee effects. Population Ecology 51:355–372.

Gibbs PE. 2014. Late-acting self-incompatibility – the pariah breeding system in flowering plants. New Phytologist 203:717–734.

Gilbert KJ, Peischl S, Excoffier L. 2018. Mutation load dynamics during environmentally-driven range shifts.Bomblies K, editor. PLOS Genetics 14:e1007450.

Gilbert KJ, Sharp NP, Angert AL, Conte GL, Draghi JA, Guillaume F, Hargreaves AL, Matthey-Doret R, Whitlock MC. 2017. Local Adaptation Interacts with Expansion Load during Range Expansion: Maladaptation Reduces Expansion Load. The American Naturalist 189:368–380.

Glémin S, Ronfort J. 2013. Adaptation and Maladaptation in Selfing and Outcrossing Species: New Mutations Versus Standing Variation. Evolution 67:225–240.

Goodwillie C, Kalisz S, Eckert CG. 2005. The Evolutionary Enigma of Mixed Mating Systems in Plants: Occurrence, Theoretical Explanations, and Empirical Evidence. Annual Review of Ecology, Evolution, and Systematics 36:47–79.

Goudet J. 1995. FSTAT (Version 1.2): A Computer Program to Calculate F-Statistics. Journal of Heredity 86:485–486.

Goudet J. 2005. hierfstat, a package for r to compute and test hierarchical F-statistics. Molecular Ecology Notes 5:184–186.

Goudet J, Jombart T. 2015. hierfstat: Estimation and Tests of Hierarchical F-statistics. R package version 0.04-22. Available from: https://CRAN.R-project.org/package=hierfstat

Griffin PC, Willi Y. 2014. Evolutionary shifts to self-fertilisation restricted to geographic range margins in North American Arabidopsis lyrata. Ecology Letters 17:484–490.

Grossenbacher D, Runquist RB, Goldberg EE, Brandvain Y. 2015. Geographic range size is predicted by plant mating system. Ecology Letters 18:706–713.

Guo Y-L, Bechsgaard JS, Slotte T, Neuffer B, Lascoux M, Weigel D, Schierup MH. 2009. Recent speciation of Capsella rubella from Capsella grandiflora, associated with loss of self-incompatibility and an extreme bottleneck. Proceedings of the National Academy of Sciences 106:5246–5251.

Hallatschek O, Hersen P, Ramanathan S, Nelson DR. 2007. Genetic drift at expanding frontiers promotes gene segregation. Proceedings of the National Academy of Sciences 104:19926–19930.

Hämälä T, Mattila TM, Leinonen PH, Kuittinen H, Savolainen O. 2017. Role of seed germination in adaptation and reproductive isolation in Arabidopsis lyrata. Molecular Ecology 26:3484–3496.

Hämälä T, Mattila TM, Savolainen O. 2018. Local adaptation and ecological differentiation under selection, migration, and drift in Arabidopsis lyrata. Evolution 72:1373–1386.

Hämälä T, Savolainen O. 2019. Genomic patterns of local adaptation under gene flow in Arabidopsis lyrata. Mol Biol Evol. msz149, https://doi.org/10.1093/molbev/msz149

Hamilton MB. 2009. Population Genetics. Chichester, UK; Hoboken, NJ: Wiley-Blackwell

Henry RC, Barto KA, Travis JMJ. 2015. Mutation accumulation and the formation of range limits. Biology Letters 11:20140871–20140871.

Hewitt G. 2000. The genetic legacy of the Quaternary ice ages. Nature 405:907–913.

Hohmann N, Wolf EM, Lysak MA, Koch MA. 2015. A Time-Calibrated Road Map of Brassicaceae Species Radiation and Evolutionary History. The Plant Cell:tpc.15.00482.

Huber CD, Durvasula A, Hancock AM, Lohmueller KE. 2018. Gene expression drives the evolution of dominance. Nature Communications 9:2750.

Huber CD, Nordborg M, Hermisson J, Hellmann I. 2014. Keeping It Local: Evidence for Positive Selection in Swedish Arabidopsis thaliana. Mol Biol Evol 31:3026–3039.

Hudson RR. 2002. Generating samples under a Wright-Fisher neutral model of genetic variation. Bioinformatics 18:337–338.

Hudson RR, Wayne MS. 1992. Estimation of Levels of Gene FlowFrom DNA Sequence Data. 132:583–589.

Ingvarsson P. 2002. A Metapopulation Perspective on Genetic Diversity and Differentiation in Partially Self-Fertilizing Plants. Evolution 56:2368–2373.

Jain SK. 1976. The Evolution of Inbreeding in Plants. Annual Review of Ecology and Systematics 7:469–495.

Jensen JD, Thornton KR, Bustamante CD, Aquadro CF. 2007. On the Utility of Linkage Disequilibrium as a Statistic for Identifying Targets of Positive Selection in Nonequilibrium Populations. Genetics 176:2371–2379.

Jombart T. 2008. adegenet: a R package for the multivariate analysis of genetic markers. Bioinformatics 24:1403–1405.

Juric I, Aeschbacher S, Coop G. 2016. The Strength of Selection against Neanderthal Introgression. PLOS Genetics 12:e1006340.

Kärkkäinen K, Kuittinen H, Treuren R van, Vogl C, Oikarinen S, Savolainen O. 1999. Genetic Basis of Inbreeding Depression in Arabis Petraea. Evolution 53:1354–1365.

Klopfstein S, Currat M, Excoffier L. 2006. The Fate of Mutations Surfing on the Wave of a Range Expansion. Molecular Biology and Evolution 23:482–490.

Koch MA. 2019. The plant model system Arabidopsis set in an evolutionary, systematic, and spatio-temporal context. J Exp Bot 70:55–67.

Kopelman NM, Mayzel J, Jakobsson M, Rosenberg NA, Mayrose I. 2015. Clumpak: a program for identifying clustering modes and packaging population structure inferences across K. Mol Ecol Resour 15:1179–1191.

Korneliussen TS, Albrechtsen A, Nielsen R. 2014. ANGSD: Analysis of Next Generation Sequencing Data. BMC Bioinformatics 15:356.

Kremling KAG, Chen S-Y, Su M-H, Lepak NK, Romay MC, Swarts KL, Lu F, Lorant A, Bradbury PJ, Buckler ES. 2018. Dysregulation of expression correlates with rare-allele burden and fitness loss in maize. Nature 555:520–523.

Laenen B, Tedder A, Nowak MD, Toräng P, Wunder J, Wötzel S, Steige KA, Kourmpetis Y, Odong T, Drouzas AD, et al. 2018. Demography and mating system shape the genome-wide impact of purifying selection in *Arabis alpina*. Proceedings of the National Academy of Sciences 115:816–821.

Lamesch P, Berardini TZ, Li D, Swarbreck D, Wilks C, Sasidharan R, Muller R, Dreher K, Alexander DL, Garcia-Hernandez M, et al. 2012. The Arabidopsis Information Resource (TAIR): improved gene annotation and new tools. Nucleic Acids Research 40:D1202–D1210.

Leinonen PH, Sandring S, Quilot B, Clauss MJ, Mitchell-Olds T, Agren J, Savolainen O. 2009. Local adaptation in European populations of Arabidopsis lyrata (Brassicaceae). American Journal of Botany 96:1129–1137.

Levin DA. 2010. Environment-enhanced self-fertilization: implications for niche shifts in adjacent populations. Journal of Ecology 98:1276–1283.

Louthan AM, Doak DF, Angert AL. 2015. Where and When do Species Interactions Set Range Limits? Trends in Ecology & Evolution 30:780–792.

Lynch M. 2007. The Origins Of Genome Architecture. 1 edition. Sinauer Associates Inc

Mable BK, Dart AVR, Berardo CD, Witham L. 2005. Breakdown of Self-Incompatibility in the Perennial Arabidopsis Lyrata (brassicaceae) and Its Genetic Consequences. Evolution 59:1437–1448.

Marsaglia G, Tsang WW, Wang J. 2003. Evaluating Kolmogorov's Distribution. Journal of Statistical Software 8:1–4.

Mattila TM, Aalto EA, Toivainen T, Niittyvuopio A, Piltonen S, Kuittinen H, Savolainen O. 2016. Selection for population-specific adaptation shaped patterns of variation in the photoperiod pathway genes in Arabidopsis lyrata during post-glacial colonization. Molecular Ecology 25:581–597.

Mattila TM, Tyrmi J, Pyhäjärvi T, Savolainen O. 2017. Genome-Wide Analysis of Colonization History and Concomitant Selection in Arabidopsis lyrata. Mol Biol Evol 34:2665–2677.

Morgan MT, Wilson WG, Knight TM. 2005. Plant Population Dynamics, Pollinator Foraging, and the Selection of Self-Fertilization. The American Naturalist 166:169–183.

Muller M-H, Leppälä J, Savolainen O. 2008. Genome-wide effects of postglacial colonization in Arabidopsis lyrata. Heredity 100:47–58.

Ossowski S, Schneeberger K, Lucas-Lledó JI, Warthmann N, Clark RM, Shaw RG, Weigel D, Lynch M. 2010. The Rate and Molecular Spectrum of Spontaneous Mutations in Arabidopsis thaliana. Science 327:92–94.

Pavlidis P, Živković D, Stamatakis A, Alachiotis N. 2013. SweeD: Likelihood-Based Detection of Selective Sweeps in Thousands of Genomes. Molecular Biology and Evolution 30:2224–2234.

Peischl S, Dupanloup I, Kirkpatrick M, Excoffier L. 2013. On the accumulation of deleterious mutations during range expansions. Molecular Ecology 22:5972–5982.

Peischl S, Kirkpatrick M, Excoffier L. 2015. Expansion Load and the Evolutionary Dynamics of a Species Range. The American Naturalist 185:E81–E93.

Pfeifer B, Wittelsbürger U, Ramos-Onsins SE, Lercher MJ. 2014. PopGenome: An Efficient Swiss Army Knife for Population Genomic Analyses in R. Molecular Biology and Evolution 31:1929–1936.

Pujol B, Zhou S-R, Sanchez Vilas J, Pannell JR. 2009. Reduced inbreeding depression after species range expansion. Proceedings of the National Academy of Sciences 106:15379–15383.

Purcell S, Neale B, Todd-Brown K, Thomas L, Ferreira MAR, Bender D, Maller J, Sklar P, de Bakker PIW, Daly MJ, et al. 2007. PLINK: A Tool Set for Whole-Genome Association and Population-Based Linkage Analyses. The American Journal of Human Genetics 81:559–575.

Pyhäjärvi T, Aalto E, Savolainen O. 2012. Time scales of divergence and speciation among natural populations and subspecies of *Arabidopsis lyrata* (Brassicaceae). American Journal of Botany 99:1314–1322.

Pyhäjärvi T, García-Gil MR, Knürr T, Mikkonen M, Wachowiak W, Savolainen O. 2007. Demographic History Has Influenced Nucleotide Diversity in European Pinus sylvestris Populations. Genetics 177:1713–1724.

Quilot-Turion B, Leppälä J, Leinonen PH, Waldmann P, Savolainen O, Kuittinen H. 2013. Genetic changes in flowering and morphology in response to adaptation to a high-latitude environment in Arabidopsis lyrata. Annals of Botany 111:957–968.

R Core Team. 2018. R: A language and environment for statistical computing. R Foundation for Statistical Computing, Vienna, Austria. Available from: http://www.R-project.org/

Ross-Ibarra J, Wright SI, Foxe JP, Kawabe A, DeRose-Wilson L, Gos G, Charlesworth D, Gaut BS. 2008. Patterns of Polymorphism and Demographic History in Natural Populations of Arabidopsis lyrata.Fay JC, editor. PLoS ONE 3:e2411.

Sandring S, Riihimäki M-A, Savolainen O, Ågren J. 2007. Selection on flowering time and floral display in an alpine and a lowland population of Arabidopsis lyrata. Journal of Evolutionary Biology 20:558–567.

Savolainen O, Lascoux M, Merilä J. 2013. Ecological genomics of local adaptation. Nat Rev Genet 14:807–820.

Schierup MH. 1998. The Number of Self-Incompatibility Alleles in a Finite, Subdivided Population. 149:1153–1162.

Schierup MH, Bechsgaard JS, Christiansen FB. 2008. Selection at Work in Self-Incompatible Arabidopsis lyrata. II. Spatial Distribution of S Haplotypes in Iceland. Genetics 180:1051–1059.

Simons YB, Sella G. 2016. The impact of recent population history on the deleterious mutation load in humans and close evolutionary relatives. Current Opinion in Genetics & Development 41:150–158.

Slatkin M. 1995. A measure of population subdivision based on microsatellite allele frequencies. Genetics 139:457–462.

Slatkin M, Excoffier L. 2012. Serial Founder Effects During Range Expansion: A Spatial Analog of Genetic Drift. Genetics 191:171–181.

Sletvold N, Mousset M, Hagenblad J, Hansson B, Ågren J. 2013. Strong Inbreeding Depression in Two Scandinavian Populations of the Self-Incompatible Perennial Herb Arabidopsis Lyrata. Evolution 67:2876–2888.

Slotte T, Hazzouri KM, Ågren JA, Koenig D, Maumus F, Guo Y-L, Steige K, Platts AE, Escobar JS, Newman LK, et al. 2013. The Capsella rubella genome and the genomic consequences of rapid mating system evolution. Nat Genet 45:831–835.

Stephan W. 2016. Signatures of positive selection: from selective sweeps at individual loci to subtle allele frequency changes in polygenic adaptation. Mol Ecol 25:79–88.

Subramanian A, Tamayo P, Mootha VK, Mukherjee S, Ebert BL, Gillette MA, Paulovich A, Pomeroy SL, Golub TR, Lander ES, et al. 2005. Gene set enrichment analysis: A knowledge-based

approach for interpreting genome-wide expression profiles. Proceedings of the National Academy of Sciences 102:15545–15550.

Tataru P, Bataillon T. 2019. polyDFEv2.0: testing for invariance of the distribution of fitness effects within and across species. Bioinformatics:1–2.

Toivainen T, Pyhäjärvi T, Niittyvuopio A, Savolainen O. 2014. A recent local sweep at the PHYA locus in the Northern European Spiterstulen population of Arabidopsis lyrata. Molecular Ecology 23:1040–1052.

Tsuchimatsu T, Kaiser P, Yew C-L, Bachelier JB, Shimizu KK. 2012. Recent Loss of Self-Incompatibility by Degradation of the Male Component in Allotetraploid Arabidopsis kamchatica.Mauricio R, editor. PLoS Genetics 8:e1002838.

Vekemans X, Poux C, Goubet PM, Castric V. 2014. The evolution of selfing from outcrossing ancestors in Brassicaceae: what have we learned from variation at the *S*- locus? Journal of Evolutionary Biology 27:1372–1385.

Vergeer P, Kunin WE. 2013. Adaptation at range margins: common garden trials and the performance of Arabidopsis lyrata across its northwestern European range. New Phytologist 197:989–1001.

Wakeley J. 1996. The Variance of Pairwise Nucleotide Differences in Two Populations with Migration. Theoretical Population Biology 49:39–57.

Willi Y, Fracassetti M, Zoller S, Van Buskirk J. 2018. Accumulation of Mutational Load at the Edges of a Species Range. Molecular Biology and Evolution 35:781–791.

Willi Y, Griffin P, Van Buskirk J. 2013. Drift load in populations of small size and low density. Heredity 110:296–302.

Wos G, Willi Y. 2018. Genetic differentiation in life history traits and thermal stress performance across a heterogeneous dune landscape in Arabidopsis lyrata. Ann Bot 122:473–484.

Wright SI, Lauga B, Charlesworth D. 2003. Subdivision and haplotype structure in natural populations of Arabidopsis lyrata. Molecular Ecology 12:1247–1263.

Zhang C, Dong S-S, Xu J-Y, He W-M, Yang T-L. 2019. PopLDdecay: a fast and effective tool for linkage disequilibrium decay analysis based on variant call format files.Schwartz R, editor. Bioinformatics 35:1786–1788.